

**The Gravitational Field of a Plane Slab**

RICARDO E. GAMBOA SARAVÍ

*Departamento de Física, Facultad de Ciencias Exactas,  
Universidad Nacional de La Plata and IFLP, CONICET.  
C.C. 67, 1900 La Plata, Argentina,  
quique@fisica.unlp.edu.ar*

Received Day Month Year

Revised Day Month Year

We discuss the exact solution of Einstein's equation corresponding to a static and plane symmetric distribution of matter with constant positive density located below  $z = 0$  matched to vacuum solutions. The internal solution depends essentially on two constants: the density  $\rho$  and a parameter  $\kappa$ . We show that these space-times finish down below at an inner singularity at finite depth  $d \leq \sqrt{\frac{\pi}{24\rho}}$ . We show that for  $\kappa \geq 0.3513\dots$ , the dominant energy condition is satisfied all over the space-time.

We match these singular solutions to the vacuum one and compute the external gravitational field in terms of slab's parameters. Depending on the value of  $\kappa$ , these slabs are either attractive, repulsive or neutral. The external solution turns out to be a Rindler's space-time. Repulsive slabs explicitly show how negative, but finite pressure can dominate the attraction of the matter. In this case, the presence of horizons in the vacuum shows that there are null geodesics which never reach the surface of the slab.

We also consider a static and plane symmetric non-singular distribution of matter with constant positive density  $\rho$  and thickness  $d$  ( $0 < d < \sqrt{\frac{\pi}{24\rho}}$ ) surrounded by two external vacuums. We explicitly write down the pressure and the external gravitational fields in terms of  $\rho$  and  $d$ . The solution turns out to be attractive and remarkably asymmetric: the "upper" solution is Rindler's vacuum, whereas the "lower" one is the singular part of Taub's plane symmetric solution. Inside the slab, the pressure is positive and bounded, presenting a maximum at an asymmetrical position between the boundaries. We show that if  $0 < \sqrt{6\pi\rho}d < 1.527\dots$ , the dominant energy condition is satisfied all over the space-time. We also show how the mirror symmetry is restored at the Newtonian limit.

We also find thinner repulsive slabs by matching a singular slice of the inner solution to the vacuum.

We also discuss solutions in which an attractive slab and a repulsive one, and two neutral ones are joined. We also discuss how to assemble a "gravitational capacitor" by inserting a slice of vacuum between two such slabs.

**1. Introduction**

Due to the complexity of Einstein's field equations, one cannot find exact solutions except in spaces of rather high symmetry, but very often with no direct physical application. Nevertheless, exact solutions can give an idea of the qualitative features that could arise in General Relativity, and so, of possible properties of realistic

2 *Ricardo E. Gamboa Saraví*

solutions of the field equations.

We have recently discussed exact solutions of Einstein's equation presenting an *empty* (free of matter) singular repelling boundary<sup>1,2</sup>. These singularities are not the sources of the fields, but they arise owing to the attraction of distant matter.

In this paper, we want to illustrate this and other curious features of relativistic gravitation by means of a simple exact solution: the gravitational field of a static plane symmetric relativistic perfect incompressible fluid with positive density located below  $z = 0$  matched to vacuum solutions. In reference<sup>3</sup>, we analyze in detail the properties of this internal solution, originally found by A. H. Taub<sup>4</sup> (see also<sup>5,6,7</sup>), and we find that it finishes up down below at an inner singularity at finite depth  $d$ , where  $0 < d < \sqrt{\frac{\pi}{24\rho}}$ . Depending on the value of a parameter  $\kappa$ , it turns out to be gravitational attractive ( $\kappa < \kappa_{\text{crit}}$ ), neutral ( $\kappa = \kappa_{\text{crit}}$ ) or repulsive ( $\kappa > \kappa_{\text{crit}}$ ), where  $\kappa_{\text{crit}} = 1.2143\dots$ . We also show that for  $\kappa \geq 0.3513\dots$ , the dominant energy condition is satisfied all over the space-time.

In this paper, we make a detailed analysis of the matching of these exact solutions to vacuum ones. Here, we impose the continuity of the metric components and of their first derivatives at the matching surfaces, in contrast to reference<sup>3</sup>, where not all these derivatives are continuous at the boundary.

In the first place, we consider the matching of the whole singular slabs to the vacuum, and explicitly compute the external gravitational fields in terms of the slab parameters. Repulsive slabs explicitly show how negative but finite pressure can dominate the attraction of the matter. In this case, they have the maximum depth, i.e.,  $d = \sqrt{\frac{\pi}{24\rho}}$ , and the exterior solution presents horizons showing that there are vertical photons that cannot reach the slab surface.

Secondly, we consider a non-singular slice of these slabs with thickness  $d$  ( $0 < d < \sqrt{\frac{\pi}{24\rho}}$ ) surrounded by two external vacuum. Some of the properties of this solution have already been discussed in reference<sup>6</sup>. Here, we explicitly write down the pressure and the external gravitational fields in terms of  $\rho$  and  $d$ . The solution turns out to be attractive, and remarkably asymmetric: the “upper” solution is Rindler's vacuum, whereas the “lower” one is the singular part of Taub's plane symmetric solution. Inside the slab, the pressure is positive and bounded, presenting a maximum at an asymmetrical position between the boundaries. We show that if  $0 < \sqrt{6\pi\rho}d < 1.527\dots$ , the dominant energy condition is satisfied all over the space-time. This solution finishes up down below at an empty repelling boundary where space-time curvature diverges. This exact solution clearly shows how the attraction of distant matter can shrink the space-time in such a way that it finishes at a free of matter singular boundary, as pointed out in<sup>1</sup>. We also show how the mirror symmetry is restored at the Newtonian limit.

We also construct thinner repulsive slabs by matching a singular slice of the inner solution to vacuum. These slabs turn out to be less repulsive than the ones discussed above, since all incoming vertical null geodesics reach the slab surface in

this case.

For the sake of completeness, in section 2, we include some results from reference 3 which are necessary for the computations of the following sections. In section 3, we show under which conditions the dominant energy condition is satisfied. In section 4, we discuss how solutions can be matched. In section 5, we study the matching of the whole singular interior solution to vacuum. In section 6, we match two interior solutions facing each other. In section 7, we discuss the matching of a non-singular slice of the interior solution with two different vacuums. In section 8, we show how the mirror symmetry of this solution is restored at the Newtonian limit. In section 9 we construct thinner repulsive slabs ( $d < \sqrt{\frac{\pi}{24\rho}}$ ) by matching a singular slice of the inner solution to vacuum.

Throughout this paper, we adopt the convention in which the space-time metric has signature  $(- + + +)$ , the system of units in which the speed of light  $c = 1$ , Newton's gravitational constant  $G = 1$  and  $g$  denotes gravitational field and not the determinant of the metric.

## 2. The interior solution

In this section, we consider the solution of Einstein's equation corresponding to a static and plane symmetric distribution of matter with constant positive density and plane symmetry. That is, it must be invariant under translations in the plane and under rotations around its normal. The matter we shall consider is a perfect fluid of uniform density  $\rho$ . The stress-energy tensor is

$$T_{ab} = (\rho + p) u_a u_b + p g_{ab}, \quad (1)$$

where  $u^a$  is the velocity of fluid elements.

Due to the plane symmetry and staticity, following 9 we can find coordinates  $(t, x, y, z)$  such that

$$ds^2 = -\mathcal{G}(z)^2 dt^2 + e^{2V(z)} (dx^2 + dy^2) + dz^2, \quad (2)$$

that is, the more general metric admitting the Killing vectors  $\partial_x, \partial_y, x\partial_y - y\partial_x$  and  $\partial_t$ .

The non identically vanishing components of the Einstein tensor are

$$G_{tt} = -\mathcal{G}^2 (2V'' + 3V'^2) \quad (3)$$

$$G_{xx} = G_{yy} = e^{2V} (\mathcal{G}''/\mathcal{G} + \mathcal{G}'/\mathcal{G} V' + V'' + V'^2), \quad (4)$$

$$G_{zz} = V' (2\mathcal{G}'/\mathcal{G} + V'), \quad (5)$$

where a prime ( $'$ ) denotes differentiation with respect to  $z$ .

On the other hand, due to the assumed symmetries and to the fact that the material content is a perfect fluid,  $u_a = (-\mathcal{G}, 0, 0, 0)$ , so

$$T_{ab} = \text{diag} (\rho \mathcal{G}^2, p e^{2V}, p e^{2V}, p), \quad (6)$$

4 *Ricardo E. Gamboa Saraví*

where  $p$  depends only on the  $z$ -coordinate. Thus, Einstein's equations, i.e.,  $G_{ab} = 8\pi T_{ab}$ , are

$$2V'' + 3V'^2 = -8\pi\rho, \quad (7)$$

$$\mathcal{G}''/\mathcal{G} + \mathcal{G}'/\mathcal{G} V' + V'' + V'^2 = 8\pi p, \quad (8)$$

$$V'(2\mathcal{G}'/\mathcal{G} + V') = 8\pi p. \quad (9)$$

Moreover,  $\nabla_a T^{ab} = 0$  yields

$$p' = -(\rho + p)\mathcal{G}'/\mathcal{G}. \quad (10)$$

Of course, due to Bianchi's identities equations, (7), (8), (9) and (10) are not independent, so we shall here use only (7), (9), and (10).

Since  $\rho$  is constant, from (10) we readily find

$$p = C_p/\mathcal{G}(z) - \rho, \quad (11)$$

where  $C_p$  is an arbitrary constant.

By setting  $W(z) = e^{\frac{2}{3}V(z)}$ , we can write (7) as  $W'' = -6\pi\rho W$ , and its general solution can be written as

$$W(z) = C_1 \sin(\sqrt{6\pi\rho} z + C_2), \quad (12)$$

where  $C_1$  and  $C_2$  are arbitrary constants. Therefore, we have

$$V(z) = \frac{2}{3} \ln \left( C_1 \sin(\sqrt{6\pi\rho} z + C_2) \right). \quad (13)$$

Now, by replacing (11) into (9), we get the first order linear differential equation which  $\mathcal{G}(z)$  obeys

$$\mathcal{G}' = - \left( \frac{4\pi\rho}{V'} + \frac{V'}{2} \right) \mathcal{G} + \frac{4\pi C_p}{V'} \quad (14)$$

$$= -\sqrt{6\pi\rho} \left( \tan u + \frac{1}{3} \cot u \right) \mathcal{G} + \sqrt{6\pi\rho} \frac{C_p}{\rho} \tan u, \quad (15)$$

where  $u = \sqrt{6\pi\rho} z + C_2$ . And in the last step, we have made use of (13). The general solution of (14) can be written as <sup>a</sup>

$$\begin{aligned} \mathcal{G} &= \frac{\cos u}{(\sin u)^{1/3}} \left( C_3 + \frac{C_p}{\rho} \int_0^u \frac{(\sin u')^{\frac{4}{3}}}{(\cos u')^2} du' \right) \\ &= C_3 \frac{\cos u}{(\sin u)^{\frac{1}{3}}} + \frac{3C_p}{7\rho} \sin^2 u {}_2F_1\left(1, \frac{2}{3}; \frac{13}{6}; \sin^2 u\right), \end{aligned} \quad (16)$$

where  $C_3$  is another arbitrary constant, and  ${}_2F_1(a, b; c; z)$  is the Gauss hypergeometric function (see the appendix at the end of the paper).

Therefore, the line element (2) becomes

$$ds^2 = -\mathcal{G}(z)^2 dt^2 + (C_1 \sin u)^{\frac{4}{3}} (dx^2 + dy^2) + dz^2, \quad (17)$$

<sup>a</sup>In the appendix we show how the integral appearing in the first line of (16) is performed.

where  $\mathcal{G}(z)$  is given in (16) and  $u = \sqrt{6\pi\rho} z + C_2$ . Thus, the solution contains five arbitrary constants:  $\rho$ ,  $C_p$ ,  $C_1$ ,  $C_2$ , and  $C_3$ . The range of the coordinate  $z$  depends on the value of these constants.

Notice that the metric (17) has a space-time curvature singularity where  $\sin u = 0$ , since straightforward computation of the scalar quadratic in the Riemann tensor yields

$$\begin{aligned} R_{abcd}R^{abcd} &= 4(\mathcal{G}''^2 + 2\mathcal{G}'^2 V'^2) / \mathcal{G}^2 + 4(2V''^2 + 4V''V'^2 + 3V'^4) \\ &= \frac{256}{3} \pi^2 \rho^2 \left( 2 + \sin^{-4} u + \frac{3}{4} \left( \frac{p}{\rho} + 1 \right) \left( \frac{3p}{\rho} - 1 \right) \right), \end{aligned} \quad (18)$$

so  $R_{abcd}R^{abcd} \rightarrow \infty$  when  $\sin u \rightarrow 0$ .

On the other hand, by contracting Einstein's equation, we get

$$R(z) = 8\pi(\rho - 3p(z)) = 8\pi(4\rho - 3C_p/\mathcal{G}(z)). \quad (19)$$

For  $\rho > 0$ ,  $C_p > 0$  and  $C_3 > 0$ , the solution (17) was found by Taub<sup>4,7</sup>. Nevertheless, this solution has a wider range of validity.

Of course, from this solution we can obtain vacuum ones as a limit. In fact, when  $C_p = 0$ , it is clear from (11) that  $p(z) = -\rho$ , and the solution (17) turns out to be a vacuum solution with a cosmological constant  $\Lambda = 8\pi\rho$ <sup>10,7</sup>

$$\begin{aligned} ds^2 &= -\cos^2 u \sin^{-\frac{2}{3}} u dt^2 + \sin^{\frac{4}{3}} u (dx^2 + dy^2) + dz^2, \\ -\infty < t < \infty, \quad -\infty < x < \infty, \quad -\infty < y < \infty, \quad 0 < u < \pi, \end{aligned} \quad (20)$$

where  $u = \sqrt{3\Lambda}/2 z + C_2$ . We get from (19) that it is a space-time with constant scalar curvature  $4\Lambda$ , and from (18) we get that

$$R_{abcd}R^{abcd} = \frac{4}{3} \Lambda^2 \left( 2 + \frac{1}{\sin^4 u} \right). \quad (21)$$

Now, we take the limit  $\Lambda \rightarrow 0$  ( $\rho \rightarrow 0$ ). By setting  $C_2 = \pi - \frac{\sqrt{3\Lambda}}{6g}$  and an appropriate rescaling of the coordinates  $\{t, x, y\}$ , we can readily see that, when  $\Lambda \rightarrow 0$ , (20) becomes

$$\begin{aligned} ds^2 &= -(1 - 3gz)^{-\frac{2}{3}} dt^2 + (1 - 3gz)^{\frac{4}{3}} (dx^2 + dy^2) + dz^2, \\ -\infty < t < \infty, \quad -\infty < x < \infty, \quad -\infty < y < \infty, \quad 0 < 1 - 3gz < \infty, \end{aligned} \quad (22)$$

where  $g$  is an arbitrary constant. In (22), the coordinates have been chosen in such a way that it describes a homogeneous gravitational field  $g$  pointing in the negative  $z$ -direction in a neighborhood of  $z = 0$ . The metric (22) is Taub's<sup>9</sup> vacuum plane solution expressed in the coordinates used in Ref.<sup>1</sup>, where a detailed study of it can be found.

On the other hand, by setting  $C_2 = \frac{\pi}{2} + \frac{\sqrt{3\Lambda}}{2g}$  and an appropriate rescaling of the coordinate  $t$ , we can readily see that, when  $\Lambda \rightarrow 0$ , (20) becomes

$$\begin{aligned} ds^2 &= -(1 + gz)^2 dt^2 + dx^2 + dy^2 + dz^2, \\ -\infty < t < \infty, \quad -\infty < x < \infty, \quad -\infty < y < \infty, \quad -\frac{1}{g} < z < \infty, \end{aligned} \quad (23)$$

6 *Ricardo E. Gamboa Saraví*

where  $g$  is an arbitrary constant, and the coordinates have been chosen in such a way that it also describes a homogeneous gravitational field  $g$  pointing in the negative  $z$ -direction in a neighborhood of  $z = 0$ . The metric (23) is, of course, Rindler's flat space-time.

For *exotic* matter, some interesting solutions also arise, but the complete analysis turns out to be somehow involved. So, for the sake of clarity, we shall confine our attention to positive values of  $\rho$  and  $C_p \neq 0$ , leaving the complete study to a forthcoming publication <sup>11</sup>.

Now, it is clear from (7), (8), (9) and (10) that field equations are invariant under the transformation  $z \rightarrow \pm z + z_0$ , i.e.,  $z$ -translations and mirror reflections across any plane  $z = \text{const}$ . Thus, if  $\{\mathcal{G}(z), V(z), p(z)\}$  is a solution  $\{\mathcal{G}(\pm z + z_0), V(\pm z + z_0), p(\pm z + z_0)\}$  is another one, where  $z_0$  is an arbitrary constant. Therefore, taking into account that  $u = \sqrt{6\pi\rho}z + C_2$ , without loss of generality, the consideration of the case  $0 < u < \pi/2$  shall suffice.

By an appropriate rescaling of the coordinates  $\{x, y\}$ , without loss of generality, we can write the metric (17) as

$$ds^2 = -\mathcal{G}(z)^2 dt^2 + \sin^{\frac{4}{3}} u (dx^2 + dy^2) + dz^2, \\ -\infty < t < \infty, \quad -\infty < x < \infty, \quad -\infty < y < \infty, \quad 0 < u = \sqrt{6\pi\rho}z + C_2 \leq \pi/2, \quad (24)$$

and (16) as

$$\mathcal{G}(z) = \frac{\kappa C_p}{\rho} \frac{\cos u}{\sin^{\frac{1}{3}} u} + \frac{3C_p}{7\rho} \sin^2 u {}_2F_1\left(1, \frac{2}{3}; \frac{13}{6}; \sin^2 u\right), \quad (25)$$

where  $\kappa$  is an arbitrary constant.

By replacing (25) into (11), we see that the pressure is independent of  $C_p$ . On the other hand, since  $\mathcal{G}(z)$  appears squared in (24), it suffices to consider  $C_p > 0$ . Therefore, rescaling the coordinate  $t$ , we may set  $C_p = \rho$ . Thus, (25) becomes

$$\mathcal{G}(z) = G_\kappa(u) = \kappa \frac{\cos u}{\sin^{1/3} u} + \frac{3}{7} \sin^2 u {}_2F_1\left(1, \frac{2}{3}; \frac{13}{6}; \sin^2 u\right), \quad (26)$$

where  $G_\kappa(u)$  is defined for future use, and we recall that  $u = \sqrt{6\pi\rho}z + C_2$ . Furthermore, (11) becomes

$$p(z) = \rho(1/\mathcal{G}(z) - 1). \quad (27)$$

Therefore, the solution depends on two essential parameters,  $\rho$  and  $\kappa$ . We shall discuss in detail the properties of the functions  $\mathcal{G}(z)$  and  $p(z)$  depending on the value of the constant  $\kappa$ .

By using the transformation (93), we can write  $\mathcal{G}(z)$  as

$$\mathcal{G}(z) = \frac{(\kappa - \kappa_{\text{crit}}) \cos u + {}_2F_1\left(-\frac{1}{2}, -\frac{1}{6}; \frac{1}{2}; \cos^2 u\right)}{\sin^{1/3} u}, \quad (28)$$

where

$$\kappa_{\text{crit}} = \frac{\sqrt{\pi}\Gamma(7/6)}{\Gamma(2/3)} = 1.2143\dots, \quad (29)$$

which is the form used in references <sup>5,6</sup>, and which is more suitable to analyze its properties near  $u = \pi/2$ .

Now, the hypergeometric function in (26) is a monotonically increasing continuous positive function of  $u$  for  $0 \leq u \leq \pi/2$ , since  $c - a - b = 1/2 > 0$ . Furthermore, taking into account that  ${}_2F_1(a, b; c; 0) = 1$  and (93), we have

$${}_2F_1\left(1, \frac{2}{3}; \frac{13}{6}; 0\right) = 1, \quad \text{and} \quad {}_2F_1\left(1, \frac{2}{3}; \frac{13}{6}; 1\right) = \frac{7}{3}. \quad (30)$$

Therefore, we readily see from (26) that, no matter what the value of  $\kappa$  is,  $\mathcal{G}(z)|_{u=\pi/2} = 1$ , and we get then from (27) that  $p(z)$  vanishes at  $u = \pi/2$ . On the other hand, since

$$\mathcal{G}(z) = \kappa u^{-\frac{1}{3}} + O(u^{\frac{5}{3}}) \quad \text{as} \quad u \rightarrow 0, \quad (31)$$

$\mathcal{G}(z)|_{u=0} = 0$  if  $\kappa = 0$ , whereas it diverges if  $\kappa \neq 0$ .

For the sake of clarity, we shall analyze separately the cases  $\kappa > 0$ ,  $\kappa = 0$ , and  $\kappa < 0$ .

### 2.1. $\kappa > 0$

In this case, it is clear from (26) that  $\mathcal{G}(z)$  is positive definite when  $0 < u \leq \pi/2$ . On the other hand, from (8) and (9), we get

$$\mathcal{G}'' = \mathcal{G}'V' - \mathcal{G}V'' = -\left(V'' + \frac{V'^2}{2} + 4\pi\rho\right)\mathcal{G} + 4\pi C_p = V'^2\mathcal{G} + 4\pi\rho, \quad (32)$$

where we have made use of (14), (7) and  $C_p = \rho$ . Then, also  $\mathcal{G}''$  is positive definite in  $0 < u \leq \pi/2$ , and so  $\mathcal{G}'$  is a monotonically increasing continuous function of  $u$  in this interval.

Now, taking into account that  $\mathcal{G}' = \partial_z \mathcal{G} = \sqrt{6\pi\rho} \partial_u \mathcal{G}$ , we get from (26) that

$$\mathcal{G}'(z) = -\frac{\kappa\sqrt{6\pi\rho}}{3}u^{-\frac{4}{3}} + O(u^{\frac{2}{3}}) \quad \text{as} \quad u \rightarrow 0, \quad (33)$$

and from (28) that

$$\mathcal{G}'(z)|_{u=\pi/2} = \sqrt{6\pi\rho}(\kappa_{\text{crit}} - \kappa). \quad (34)$$

If  $\kappa \geq \kappa_{\text{crit}}$ ,  $\mathcal{G}'$  is negative for small enough values of  $u$  and non-positive at  $u = \pi/2$ . Hence  $\mathcal{G}'$  is negative in  $0 < u < \pi/2$ , so  $\mathcal{G}(z)$  is decreasing, and then  $\mathcal{G}(z) > \mathcal{G}(z)|_{u=\pi/2} = 1$  in this interval (see Fig.1(a) and Fig.1(b)).

For  $\kappa_{\text{crit}} > \kappa > 0$ ,  $\mathcal{G}'$  is negative for sufficiently small values of  $u$  and positive at  $\pi/2$ . So, there is one (and only one) value  $u_m$  where it vanishes. Clearly  $\mathcal{G}(z)$  attains a local minimum there. Hence, there is one (and only one) value  $u_0$  ( $0 < u_0 < \pi/2$ ) such that  $\mathcal{G}(z)|_{u=u_0} = \mathcal{G}(z)|_{u=\pi/2} = 1$ , and then  $\mathcal{G}(z) < 1$  when  $u_0 < u < \pi/2$  (see Fig.1(c) and Fig.1(d)).

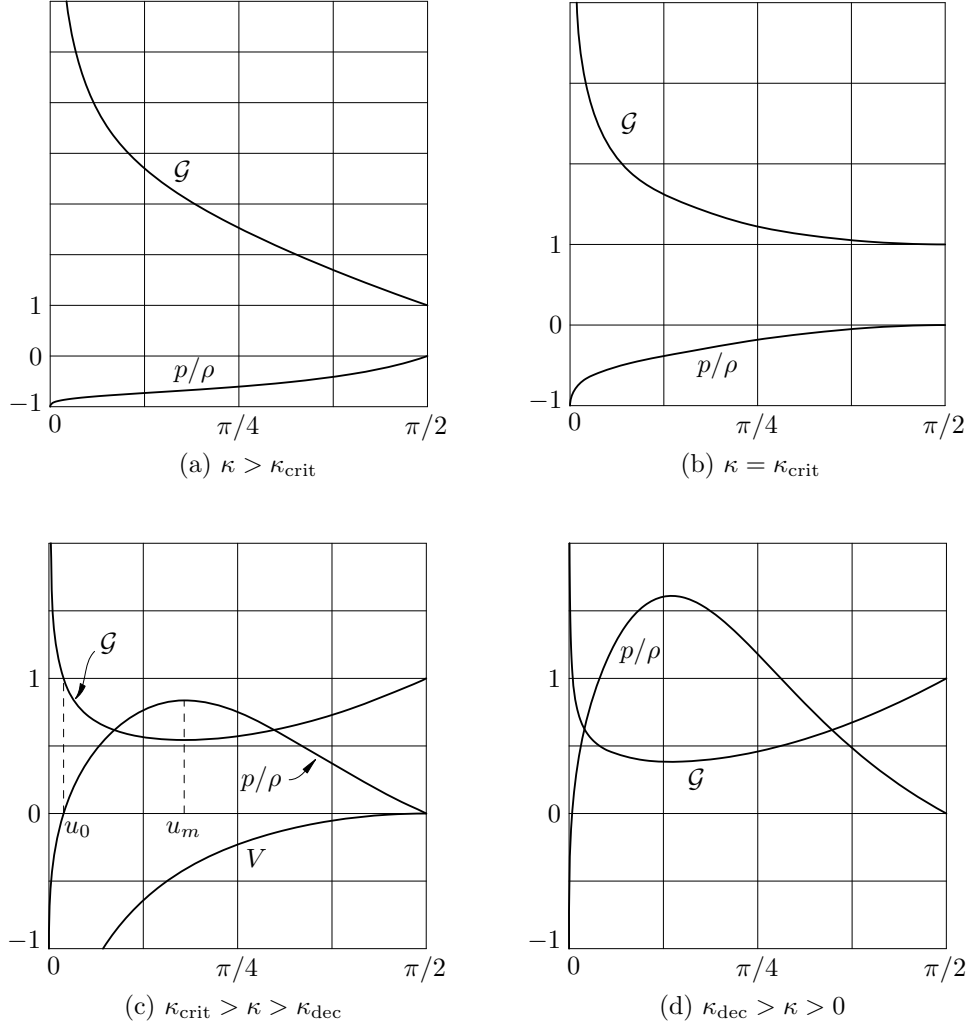
8 *Ricardo E. Gamboa Saraví*


Fig. 1.  $\mathcal{G}(z)$ ,  $V(z)$  and  $p(z)$ , as functions of  $u$  for decreasing values of  $\kappa > 0$ . Since  $V(z)$  is independent of  $\kappa$ , it is shown once.

Since  $\mathcal{G}(z) > 0$ , it is clear from (27) that  $p(z) > 0$  if  $\mathcal{G}(z) < 1$ , and  $p(z)$  reaches a maximum when  $\mathcal{G}(z)$  attains a minimum.

Therefore, for  $\kappa \geq \kappa_{\text{crit}}$ ,  $p(z)$  is negative when  $0 \leq u < \pi/2$  and it increases monotonically from  $-\rho$  to 0 and it satisfies  $|p| \leq \rho$  all over the space-time (see Fig.1(a) and Fig.1(b)).

On the other hand, for  $\kappa_{\text{crit}} > \kappa > 0$ ,  $p(z)$  grows from  $-\rho$  to a maximum positive value when  $u = u_m$  where it starts to decrease and vanishes at  $u = \pi/2$ . Thus,  $p(z)$  is negative when  $0 < u < u_0$  and positive when  $u_0 < u < \pi/2$  (see Fig.1(c) and Fig.1(d)). It can be readily seen from (26) and (27) that, as  $\kappa$  decreases from  $\kappa_{\text{crit}}$  to



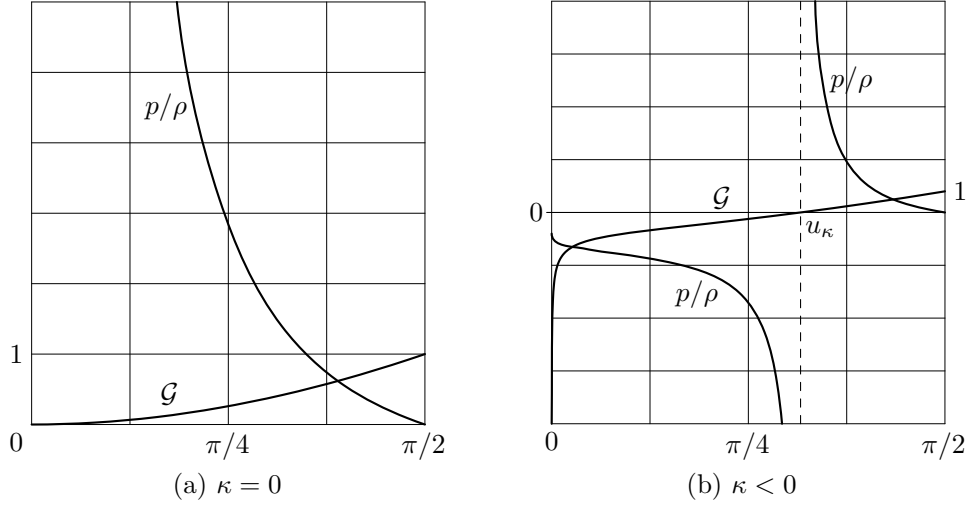


Fig. 2.  $\mathcal{G}(z)$  and  $p(z)$  as functions of  $u$  for  $\kappa \leq 0$ .

0,  $u_m$  moves to the left and the maximum value of  $p(z)/\rho$  monotonically increases from 0 to  $\infty$ . In section 3, we shall show that for  $\kappa = \kappa_{dec} = 0.3513\dots$  it gets 1, and then for  $0 < \kappa < \kappa_{dec}$ , there is a region of space-time where  $p > \rho$  and where the dominant energy condition is thus violated.

### 2.2. $\kappa = 0$

In this case, it is clear from (26) that  $\mathcal{G}$  monotonically increases with  $u$  from 0 to  $\mathcal{G}(z)|_{u=\pi/2} = 1$ . Therefore,  $p$  is a monotonically decreasing positive continuous function of  $u$  in  $0 < u < \pi/2$  (see Fig.2(a)). Furthermore, at  $u = 0$  it diverges, since

$$p(z) \sim \frac{7\rho}{3}u^{-2} \rightarrow +\infty \quad \text{as } u \rightarrow 0. \quad (35)$$

### 2.3. $\kappa < 0$

In this case, we see from (33) that  $\mathcal{G}'$  is positive when  $u$  takes small enough values, and from (34) we see that it is also positive when  $u$  is near to  $\pi/2$ .

Now, suppose that  $\mathcal{G}'(z)$  attains a local minimum when  $u = u_1$  ( $0 < u_1 < \pi/2$ ), then  $\mathcal{G}''(z)|_{u=u_1} = 0$ . Hence, we get from (32) that  $\mathcal{G}(z)|_{u=u_1} < 0$ . And taking into account that  $V'(z)|_{u=u_1} = 2\sqrt{6\pi\rho}/3 \cot u_1 > 0$ , we see from (14) that  $\mathcal{G}'(z)|_{u=u_1} > 0$ . Thus, we have shown that  $\mathcal{G}'(z)$  is a continuous positive definite function when  $0 < u \leq \pi/2$  if  $\kappa < 0$ .

Therefore, in this case,  $\mathcal{G}(z)$  is a continuous function monotonically increasing with  $u$  when  $0 < u \leq \pi/2$ . Since it is negative for sufficiently small values of  $u$  and 1 when  $u = \pi/2$  it must vanish at a unique value of  $z$  when  $u = u_\kappa$  (say). Furthermore

10 *Ricardo E. Gamboa Saraví*

$\mathcal{G}(z) < 1$  when  $0 < u < \pi/2$ . Clearly, we get from (28) that  $u_\kappa$  is given implicitly in terms of  $\kappa$  through

$$\kappa = \kappa_{\text{crit}} - \frac{{}_2F_1\left(-\frac{1}{2}, -\frac{1}{6}; \frac{1}{2}; \cos^2 u_\kappa\right)}{\cos u_\kappa \sin^{1/3} u_\kappa}. \quad (36)$$

We can readily see from (36) that  $u_\kappa$  is a monotonically decreasing function of  $\kappa$  in  $-\infty < \kappa < 0$ , and it tends to  $\pi/2$  when  $\kappa \rightarrow -\infty$  and to 0 when  $\kappa \rightarrow 0^-$ .

From (27), it is clear that  $p(z)$  diverges when  $u = u_\kappa$ . Furthermore, (27) also shows that  $p(z) < 0$  when  $\mathcal{G}(z) < 0$ . And taking into account that  $\mathcal{G}(z) < 1$ , we see that  $p(z) > 0$  when  $\mathcal{G}(z) > 0$ . Therefore,  $p(z)$  is negative when  $0 < u < u_\kappa$  whereas it is positive when  $u_\kappa < u < \pi/2$  (see Fig.2(b)).

On the other hand, we see from (18) that, when  $\kappa$  is negative, another space-time curvature singularity arises at  $u_\kappa$  (besides the one at  $u = 0$ ) since  $p$  diverges there.

Therefore, if  $\kappa$  is negative, the metric (24) describes two very different space-times:

(a) For  $0 < u < u_\kappa$ , the whole space-time is trapped between two singularities separated by a finite distance  $\sqrt{6\pi\rho}u_\kappa$ . This is a space-time full of a fluid with constant positive density  $\rho$  and negative pressure  $p$  monotonically decreasing with  $u$ , and  $p(z)|_{u=0} = -\rho$  and  $p(z) \rightarrow -\infty$  as  $u \rightarrow u_\kappa$ .

(b) For  $u_\kappa < u < \pi/2$ , the pressure is positive and monotonically decreasing with  $u$ ,  $p(z) \rightarrow \infty$  as  $u \rightarrow u_\kappa$  and  $p(z)|_{u=\pi/2} = 0$ .

### 3. The maximum of the pressure and the dominant energy condition

We have seen in the preceding section that for  $\kappa \geq \kappa_{\text{crit}}$ ,  $p(z)$  is negative, it increases monotonically from  $-\rho$  to 0 and it satisfies  $|p| \leq \rho$  all over the space-time (see Fig.1(a) and Fig.1(b)). On the other hand, for  $\kappa \leq 0$ ,  $p(z)$  is unbounded at an inner singularity and thus the dominant energy condition is not satisfied in this case.

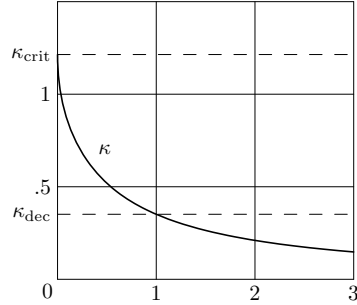
For  $\kappa_{\text{crit}} > \kappa > 0$ , since  $\mathcal{G}(z) > 0$ , it is clear from (11) that  $p(z) > 0$  if  $\mathcal{G}(z) < 1$ , and that  $p(z)$  reaches a maximum when  $\mathcal{G}(z)$  attains a minimum. Then,  $p(z)$  grows from  $-\rho$  to a maximum positive value  $p_m$  when  $u = u_m$ , where it starts to decrease and vanishes at  $u = \pi/2$ . Thus,  $-\rho \leq p(z) < 0$  for  $0 < u \leq u_0$  and  $0 < p(z) < p_m$  when  $u_0 < u < \pi/2$  (see Fig.1(c)).

We readily see from (9), since  $\mathcal{G}'(z)|_{u=u_m}$  vanishes, that

$$p_m = p(z)|_{u=u_m} = \frac{1}{8\pi} (V'(z))^2|_{u=u_m} = \frac{\rho}{3} \cot^2 u_m, \quad (37)$$

where we have made use of (13), and so the maximum value of  $p(z)$  monotonically decreases from  $\infty$  to 0 in  $0 < u_m < \pi/2$ .

Now, by replacing (37) into (28) and taking into account (27), we can write


 Fig. 3.  $\kappa$  as a function of  $p_m$ .

down  $\kappa$  in terms of  $p_m$

$$\kappa = \kappa_{\text{crit}} + \frac{(\rho + 3p_m)^{\frac{1}{2}}}{(3p_m)^{\frac{1}{2}}} \left( \frac{\rho^{\frac{7}{6}}}{(\rho + p_m)(\rho + 3p_m)^{\frac{1}{6}}} - {}_2F_1\left(-\frac{1}{2}, -\frac{1}{6}; \frac{1}{2}; \frac{3p_m}{\rho + 3p_m}\right) \right) \quad (38)$$

$$= \kappa_{\text{crit}} - 2\sqrt{\frac{p_m}{3\rho}} \left( 1 - \frac{1}{3} \frac{p_m}{\rho} + \frac{8}{21} \frac{p_m^3}{\rho^3} + \dots \right) \text{ for } p_m < \rho, \quad (39)$$

which clearly shows that  $\kappa \rightarrow \kappa_{\text{crit}}$  as  $p_m \rightarrow 0$ . On the other hand, by using (96), we can write

$$\kappa = \frac{2}{\sqrt[6]{3}} \left( \frac{\rho}{p_m} \right)^{\frac{7}{6}} \left( \frac{3}{7} - \frac{17}{39} \left( \frac{\rho}{p_m} \right) + \dots \right) \text{ for } p_m > \rho, \quad (40)$$

which clearly shows that  $\kappa \rightarrow 0$  as  $p_m \rightarrow \infty$ . Thus, as  $\kappa$  increases from 0 to  $\kappa_{\text{crit}}$ ,  $p_m$  monotonically decreases from  $\infty$  to 0 (see Fig.3).

Hence, there is a value  $\kappa_{\text{dec}}$  of  $\kappa$  for which  $p_m = \rho$ , and from (38) we see that it is given by

$$\kappa_{\text{dec}} = \kappa_{\text{crit}} + \frac{2}{\sqrt{3}} \left( \frac{1}{2\sqrt[3]{2}} - {}_2F_1\left(-\frac{1}{2}, -\frac{1}{6}; \frac{1}{2}; \frac{3}{4}\right) \right) = 0.351307\dots \quad (41)$$

Also note that, in this case, we get from (37) that the maximum of the pressure occurs at  $u_m = \pi/6$ .

Thus, for  $0 < \kappa < \kappa_{\text{dec}}$ , there is a region of space-time where  $p > \rho$  and where the dominant energy condition is thus violated. However, we see that for  $\kappa_{\text{dec}} \leq \kappa < \kappa_{\text{crit}}$ , the condition  $|p| < \rho$  is everywhere satisfied.

Therefore, the dominant energy condition is satisfied all over the space-time if  $\kappa \geq \kappa_{\text{dec}}$ .

Notice that, for  $\kappa_{\text{crit}} > \kappa > 0$ , by eliminating  $\kappa$  by means of (38), the solution can be parameterized in terms of  $p_m$  and  $\rho$ .

#### 4. The matching of solutions and the external gravitational fields

We shall discuss matching the interior solution to a vacuum one, as well as joining two interior solutions facing each other at the surfaces where the pressure vanishes. For any value of  $\kappa$ ,  $p(z) = 0$  at  $u = \pi/2$ , while for  $\kappa_{\text{crit}} > \kappa > 0$  it also vanishes at  $u = u_0$ . Therefore, the matching at  $u = \pi/2$  is always possible, while the matching at  $u = u_0$  is also possible in the latter case.

We shall impose the continuity of the metric components and of their first derivatives at the matching surfaces.

Notice that, due to the symmetry required, vacuum solutions satisfy the field equations (7), (8) and (9), with  $\rho = p = 0$ . In this case, we immediately get from (9) that or  $V' = 0$  or  $2 \mathcal{G}'/\mathcal{G} + V' = 0$ .

In the former case, we get from (8) that  $\mathcal{G}'' = 0$ , and the solution is

$$ds^2 = -(A + Bz)^2 dt^2 + C(dx^2 + dy^2) + dz^2, \quad (42)$$

which is the Rindler space-time.

In the latter one, it can be written as

$$ds^2 = -(A + Bz)^{-\frac{2}{3}} dt^2 + C(A + Bz)^{\frac{4}{3}} (dx^2 + dy^2) + dz^2, \quad (43)$$

which is the Taub's vacuum plane solution<sup>9</sup>.

Therefore, as pointed out by the authors of reference<sup>6</sup>, if at the matching "plane" the interior  $V'$  vanishes, we can only match it to Rindler's space-time, since for the Taub's one  $V'$  does not vanish at any finite point. Whereas, if on the contrary,  $V'$  does not vanish at the matching "plane", we can only match the inner solution with Taub's one, since for Rindler's one,  $V'$  vanishes anywhere.

Now, we see from (13) that  $V'$  vanishes at  $u = \pi/2$  and it is non zero at  $u = u_0 \neq \pi/2$ . Therefore the solution can be matched to Rindler's space-time at  $u = \pi/2$  and to Taub's vacuum plane solution at  $u = u_0$ .

Notice that in reference<sup>3</sup> we did not demand the continuity of  $V'(z)$  at the matching surface and we analyzed there the matching of the solution to Taub's vacuum plane solution at  $u = \pi/2$ .

In the next section, we discuss the matching of the whole interior solution to Rindler vacuum, for any value of  $\kappa$  at  $u = \pi/2$ , while we match two interior solutions facing each other at  $u = \pi/2$  in section 6.

In section 7, for  $\kappa_{\text{crit}} > \kappa > 0$ , we discuss the matching of the slice of the interior solution  $u_0 \leq u \leq \pi/2$  with both vacua, while, in section 9 we match the remaining piece (i.e.  $0 < u < u_0$ ) to a Taub's vacuum.

#### 5. Matching the whole slab to a Rindler space-time

In this section, we discuss matching the whole interior solution to a vacuum one at  $u = \pi/2$ .

Since the field equations are invariant under  $z$ -translation, we can choose to match the solutions at  $z = 0$  without losing generality. So we select  $C_2 = \pi/2$ , and

then (28) becomes

$$\begin{aligned} \mathcal{G}(z) &= G_\kappa(\sqrt{6\pi\rho}z + \pi/2) \\ &= \frac{-(\kappa - \kappa_{\text{crit}}) \sin(\sqrt{6\pi\rho}z) + {}_2F_1\left(-\frac{1}{2}, -\frac{1}{6}; \frac{1}{2}; \sin^2(\sqrt{6\pi\rho}z)\right)}{\cos^{1/3}(\sqrt{6\pi\rho}z)}. \end{aligned} \quad (44)$$

Therefore, the metric (24) reads

$$\begin{aligned} ds^2 &= -\mathcal{G}(z)^2 dt^2 + \cos^{4/3}(\sqrt{6\pi\rho}z) (dx^2 + dy^2) + dz^2, \\ -\infty < t < \infty, \quad -\infty < x < \infty, \quad -\infty < y < \infty, \quad -\sqrt{\frac{\pi}{24\rho}} < z \leq 0. \end{aligned} \quad (45)$$

We must impose the continuity of the components of the metric at the matching boundary. Notice that  $g_{tt}(0) = -\mathcal{G}(0)^2 = -1$ ,  $g_{xx}(0) = g_{yy}(0) = 1$ , and  $p(0) = 0$ .

Furthermore, we also impose the continuity of the derivatives of the metric components at the boundary. From (34), we have

$$\partial_z g_{tt}(0)|_{\text{interior}} = -2\mathcal{G}(0)\mathcal{G}'(0) = -2\sqrt{6\pi\rho}(\kappa_{\text{crit}} - \kappa), \quad (46)$$

and, from (45) we get

$$\partial_z g_{xx}(0)|_{\text{interior}} = \partial_z g_{yy}(0)|_{\text{interior}} = -\frac{4\sqrt{6\pi\rho}}{3} \cos^{1/3}(\sqrt{6\pi\rho}z) \sin(\sqrt{6\pi\rho}z) \Big|_{z=0} = 0. \quad (47)$$

The exterior solution, i.e. for  $z \geq 0$ , is the Rindler space-time

$$\begin{aligned} ds^2 &= -(1 + gz)^2 dt^2 + dx^2 + dy^2 + dz^2, \\ -\infty < t < \infty, \quad -\infty < x < \infty, \quad -\infty < y < \infty, \quad 0 \leq z < \infty, \end{aligned} \quad (48)$$

which describes a homogeneous gravitational field  $-g$  in the vertical (i.e.,  $z$ ) direction.

Since  $g_{tt}(0)|_{\text{exterior}} = -1$  and  $g_{xx}(0)|_{\text{exterior}} = g_{yy}(0)|_{\text{exterior}} = 1$ , the continuity of the metric components is assured. And, concerning the derivatives, we have

$$\partial_z g_{xx}(z)|_{\text{exterior}} = \partial_z g_{yy}(z)|_{\text{exterior}} = 0, \quad (49)$$

which identically matches to (47).

Moreover, we readily get

$$\partial_z g_{tt}(z)|_{\text{exterior}} = -2g(1 + 2gz). \quad (50)$$

Then, by comparing it with (33), we see that the continuity of  $\partial_z g_{tt}$  at the boundary yields

$$g = \sqrt{6\pi\rho}(\kappa_{\text{crit}} - \kappa), \quad (51)$$

which relates the external gravitational field  $g$  with matter density  $\rho$  and  $\kappa$ .

Case	$\kappa$	$g$	$p(z)$	$ p  \leq \rho$	Depth	Fig.
I	$\kappa > \kappa_{\text{crit}}$	$< 0$	$-\rho \leq p(z) \leq 0$	yes	$\sqrt{\frac{\pi}{24\rho}}$	1(a)
II	$\kappa = \kappa_{\text{crit}}$	$= 0$	$-\rho \leq p(z) \leq 0$	yes	$\sqrt{\frac{\pi}{24\rho}}$	1(b)
III	$\kappa_{\text{crit}} > \kappa \geq \kappa_{\text{dec}}$	$> 0$	$-\rho \leq p(z) \leq p_m(\kappa) \leq \rho$	yes	$\sqrt{\frac{\pi}{24\rho}}$	1(c)
IV	$\kappa_{\text{dec}} > \kappa > 0$	$> 0$	$-\rho \leq p(z) \leq p_m(\kappa)$	no	$\sqrt{\frac{\pi}{24\rho}}$	1(d)
V	$0 \geq \kappa$	$> 0$	unbounded	no	$\frac{(\pi/2 - u_\kappa)}{\sqrt{6\pi\rho}}$	2

Now, by replacing  $\kappa$  from (51) into (44), we get

$$\mathcal{G}(z) = \frac{g \sin(\sqrt{6\pi\rho}z) + \sqrt{6\pi\rho} {}_2F_1\left(-\frac{1}{2}, -\frac{1}{6}; \frac{1}{2}; \sin^2(\sqrt{6\pi\rho}z)\right)}{\sqrt{6\pi\rho} \cos^{1/3}(\sqrt{6\pi\rho}z)}, \quad (52)$$

and the solution is parameterized in terms of the external gravitational field  $g$  and the density of the matter  $\rho$ .

It can readily be seen from (51) that, if  $\kappa > \kappa_{\text{crit}}$ ,  $g$  is negative and the slab turns out to be repulsive. If  $\kappa = \kappa_{\text{crit}}$  it is *gravitationally neutral*, and the exterior is one half of Minkowski's space-time. If  $\kappa < \kappa_{\text{crit}}$ , it is attractive.

If  $\kappa > 0$ , the depth of the slab is  $\sqrt{\frac{\pi}{24\rho}}$  independently of the value of  $\kappa$ . In this case, the pressure is finite anywhere, but it is negative deep below and  $p = -\rho$  at the inner singularity (see Fig.1(a), Fig.1(b) and Fig.1(c)). But, as discussed in section 3, only when  $\kappa \geq \kappa_{\text{dec}}$  is the condition  $|p| \leq \rho$  everywhere satisfied.

If  $\kappa \leq 0$ , the pressure inside the slab is always positive, and it diverges deep below at the inner singularity (see Fig.2). Its depth is

$$d = (\pi/2 - u_\kappa)/\sqrt{6\pi\rho}, \quad (53)$$

where  $u_\kappa$  ( $0 < u_\kappa < \pi/2$ ) is given implicitly in terms of  $\kappa$  through (36). By using (36), we can write  $\kappa$  in terms of  $d$

$$\kappa = \kappa_{\text{crit}} - \frac{{}_2F_1\left(-\frac{1}{2}, -\frac{1}{6}; \frac{1}{2}; \sin^2(\sqrt{6\pi\rho}d)\right)}{\sin(\sqrt{6\pi\rho}d) \cos^{1/3}(\sqrt{6\pi\rho}d)}. \quad (54)$$

Now, in this case, by using (51) we can write the external gravitational field  $g$  in terms of the matter density  $\rho$  and the depth of the slab  $d$

$$g = \frac{\sqrt{6\pi\rho}}{\sin(\sqrt{6\pi\rho}d) \cos^{1/3}(\sqrt{6\pi\rho}d)} {}_2F_1\left(-\frac{1}{2}, -\frac{1}{6}; \frac{1}{2}; \sin^2(\sqrt{6\pi\rho}d)\right). \quad (55)$$

For the sake of clearness, we summarize the properties of the solutions discussed above in Table ??.

Case	Quadrant	$T$	$Z$	$-dT^2 + dZ^2$
Attractive	I	$(z + 1/g) \sinh gt$	$(z + 1/g) \cosh gt$	$-(z + 1/g)^2 dt^2 + dz^2$
Repulsive	I and II	$(z - 1/g) \sinh gt$	$(z - 1/g) \cosh gt$	$-(z - 1/g)^2 dt^2 + dz^2$
	III	$(z - 1/g) \cosh gt$	$(z - 1/g) \sinh gt$	$-dz^2 + (z - 1/g)^2 dt^2$
	IV	$(1/g - z) \cosh gt$	$(z - 1/g) \sinh gt$	$-dz^2 + (z - 1/g)^2 dt^2$

Some remarks are in order. First, notice that the maximum depth that a slab with constant density  $\rho$  can reach is  $\sqrt{\frac{\pi}{24\rho}}$ , being the counterpart of the well-known bound  $M < 4R/9$  ( $R < \frac{1}{\sqrt{3\pi\rho}}$ ), which holds for spherical symmetry.

If we restrict ourselves to non “exotic” matter, the dominant energy condition will put aside cases IV and V, as shown in section 3. However, as already mentioned, it is satisfied for the cases I, II and III (see Fig.1(a), Fig.1(b) and Fig.1(c)). Thus, there are still attractive, neutral and repulsive solutions satisfying this condition.

In this case, we readily get from (51) the bound

$$g \leq \sqrt{6\pi\rho} (\kappa_{\text{crit}} - \kappa_{\text{dec}}) \approx 3.75 \sqrt{\rho} . \quad (56)$$

In order to analyze the geodesics in the vacuum, it is convenient to consider the transformation from Rindler’s coordinates  $t$  and  $z$  to Minkowski’s ones  $T$  and  $Z$  shown in Table ???. Notice that, for the repulsive case, four Rindler’s patches are necessary to cover the whole exterior of the slab. Also note that, in this case,  $z$  becomes the temporal coordinate in quadrants III and IV, see Fig. 4. In this coordinates, of course, the vacuum metric becomes

$$ds^2 = -dT^2 + dx^2 + dy^2 + dZ^2 . \quad (57)$$

Notice that, the “planes”  $z = \text{constant}$  correspond to the hyperbolae  $Z^2 - T^2 = \text{constant}$ , and  $t = \text{constant}$ . On the other hand, incoming vertical null geodesics are  $Z + T = \text{constant}$ , and outgoing ones are given by  $Z - T = \text{constant}$ .

For attractive slabs, we readily see from Fig. 4(a) that all incoming vertical photons finish at the surface of the slab, while all outgoing ones escape to infinite. Vertical time-like geodesics start at the surface of the slab, reach a turning point and fall down to the slab in a finite amount of coordinate time  $t$ . Notice that a particle world-line is tangent to only one hyperbola  $Z^2 - T^2 = C$ , with  $C > 1/g$ , and that the maximum value of  $z$  that it reaches is  $C - 1/g$ .

For repulsive slabs, Fig. 4(b), two horizons appear in the vacuum: the lines  $T = \pm Z$ , showing that not all the vertical null geodesics reach the surface of the slab. In fact, only vertical incoming photons coming from region IV end at the slab surface, and only the outgoing ones finishing in region III start at the slab surface. Incoming particles can reach the surface or bounce at a turning point before getting it.

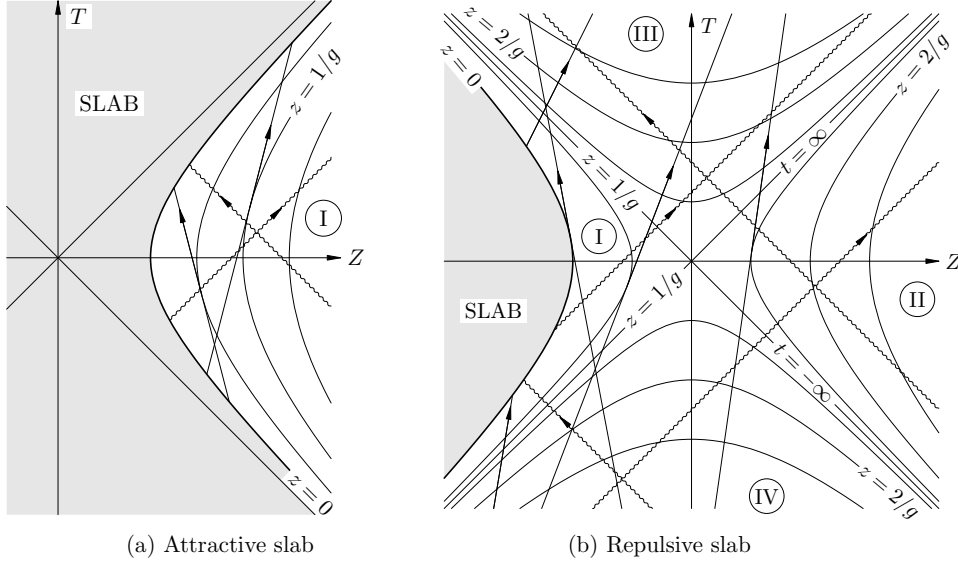


Fig. 4. Vertical time-like and null geodesics in the vacuum

## 6. Matching two slabs

Now we consider two incompressible fluids joined at  $z = 0$  where the pressure vanishes, the lower one having density  $\rho$  and the upper having density  $\rho'$ . Thus, the lower solution is given by (45). By means of the transformation  $z \rightarrow -z$ ,  $\rho \rightarrow \rho'$  and  $\kappa \rightarrow \kappa'$  we get the upper one

$$\begin{aligned}
 ds^2 = & -G_{\kappa'}(\pi/2 - \sqrt{6\pi\rho'z})^2 dt^2 + \cos^{\frac{4}{3}}(\sqrt{6\pi\rho'z})(dx^2 + dy^2) + dz^2, \\
 & -\infty < t < \infty, \quad -\infty < x < \infty, \quad -\infty < y < \infty, \quad 0 \leq z < \sqrt{\frac{\pi}{24\rho'}}. \quad (58)
 \end{aligned}$$

From (45), (47) and (58), we can readily see that  $g_{tt}(z)$ ,  $g_{xx}(z)$  and  $\partial_z g_{xx}(z)$  are continuous at  $z = 0$ . Furthermore, from (46) we see that the continuity of  $\partial_z g_{tt}$  requires

$$\sqrt{\rho}(\kappa_{\text{crit}} - \kappa) = -\sqrt{\rho'}(\kappa_{\text{crit}} - \kappa'). \quad (59)$$

Thus, if one solution has a  $\kappa$  greater than  $\kappa_{\text{crit}}$ , the other one must have it smaller than  $\kappa_{\text{crit}}$ . Therefore, the joining is only possible between an attractive solution and a repulsive one, or between two neutral ones.

It is easy to see that we can also insert a slice of arbitrary thickness of the vacuum solution (22) between them, obtaining a full relativistic plane “gravitational capacitor”. For example, we can trap a slice of Minkowski’s space-time between two solutions with  $\kappa = \kappa_{\text{crit}}$ .



## 7. Attractive Slab surrounded by two different vacuums

We have already seen that, in the case  $\kappa_{\text{crit}} > \kappa > 0$ , the pressure also vanishes inside the slab at the point where  $u = u_0$ . Here we discuss the matching of the slice of the interior solution  $u_0 \leq u \leq \pi/2$  with two vacuums.

Clearly, the thickness of the slab  $d$  is given by

$$d = \frac{(\pi/2 - u_0)}{\sqrt{6\pi\rho}}, \quad (60)$$

and  $0 < d < \sqrt{\frac{\pi}{24\rho}}$ .

Since  $\mathcal{G}(z)|_{u=u_0} = 1$ , we can write down from (28) the expression which gives  $\kappa$  in terms of  $d$  and  $\rho$

$$\kappa = \kappa_{\text{crit}} + \frac{\cos^{1/3}(\sqrt{6\pi\rho}d) - {}_2F_1\left(-\frac{1}{2}, -\frac{1}{6}; \frac{1}{2}; \sin^2(\sqrt{6\pi\rho}d)\right)}{\sin(\sqrt{6\pi\rho}d)} \quad (61)$$

$$= \kappa_{\text{crit}} - \frac{\sqrt{6\pi\rho}d}{3} \left(1 + \frac{2\pi\rho}{3}d^2 + \frac{(2\pi\rho)^2}{5}d^4 + \dots\right) \quad \text{for } \sqrt{6\pi\rho}d < 1, \quad (62)$$

which clearly shows that  $\kappa \rightarrow \kappa_{\text{crit}}$  as  $d \rightarrow 0$ . On the other hand, by using (96), we can write

$$\kappa = \frac{\cos^{1/3}(\sqrt{6\pi\rho}d)}{\sin(\sqrt{6\pi\rho}d)} \left(1 - \frac{3}{7}\cos^2(\sqrt{6\pi\rho}d) + \dots\right) \quad (63)$$

which clearly shows that  $\kappa \rightarrow 0$  as  $d \rightarrow \sqrt{\frac{\pi}{24\rho}}$ . Thus, as  $d$  increases from 0 to  $\sqrt{\frac{\pi}{24\rho}}$ ,  $\kappa$  monotonically decreases from  $\kappa_{\text{crit}}$  to 0 (see Fig.5).

Therefore, the maximum thickness  $d_{\text{dec}}$  that a solution satisfying the dominant energy condition can have, satisfies

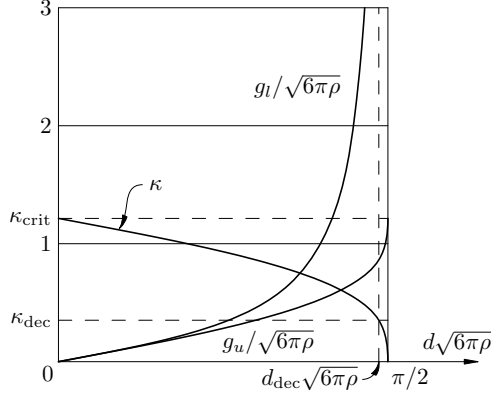
$$\kappa_{\text{dec}} = \kappa_{\text{crit}} + \frac{\cos^{1/3}(\sqrt{6\pi\rho}d_{\text{dec}}) - {}_2F_1\left(-\frac{1}{2}, -\frac{1}{6}; \frac{1}{2}; \sin^2(\sqrt{6\pi\rho}d_{\text{dec}})\right)}{\sin(\sqrt{6\pi\rho}d_{\text{dec}})}. \quad (64)$$

A straightforward numerical computation gives  $\sqrt{6\pi\rho}d_{\text{dec}} = 1.52744\dots$ . Therefore, if  $0 < d < d_{\text{dec}}$ , the dominant energy condition is satisfied anywhere. Whereas if  $d_{\text{dec}} < d < \sqrt{\frac{\pi}{24\rho}}$ , there is a region inside the slab where  $p(z) > \rho$ .

Now, by eliminating  $\kappa$  by means of (61), the solution can be parameterized in terms of  $d$  and  $\rho$ , and (44) becomes

$$\begin{aligned} \mathcal{G}(z) = & \frac{{}_2F_1\left(-\frac{1}{2}, -\frac{1}{6}; \frac{1}{2}; \sin^2(\sqrt{6\pi\rho}z)\right)}{\cos^{1/3}(\sqrt{6\pi\rho}z)} - \frac{\cos^{1/3}(\sqrt{6\pi\rho}d)}{\sin(\sqrt{6\pi\rho}d)} \frac{\sin(\sqrt{6\pi\rho}z)}{\cos^{1/3}(\sqrt{6\pi\rho}z)} \\ & + \frac{{}_2F_1\left(-\frac{1}{2}, -\frac{1}{6}; \frac{1}{2}; \sin^2(\sqrt{6\pi\rho}d)\right)}{\sin(\sqrt{6\pi\rho}d)} \frac{\sin(\sqrt{6\pi\rho}z)}{\cos^{1/3}(\sqrt{6\pi\rho}z)}. \quad (65) \end{aligned}$$

Notice that it clearly shows that  $\mathcal{G}(-d) = \mathcal{G}(0) = 1$ . By means of (27) and (65)  $p(z)$  can also be explicitly written down in terms of  $d$  and  $\rho$ . The inner line element (45)


 Fig. 5.  $\kappa$ ,  $g_u$  and  $g_l$  as functions of  $d$ .

reads

$$ds^2 = -\mathcal{G}(z)^2 dt^2 + \cos^{\frac{4}{3}}(\sqrt{6\pi\rho}z)(dx^2 + dy^2) + dz^2, \\ -\infty < t < \infty, \quad -\infty < x < \infty, \quad -\infty < y < \infty, \quad -\sqrt{\frac{\pi}{24\rho}} < -d \leq z \leq 0. \quad (66)$$

We must impose the continuity of the components of the metric and their first derivatives at both matching boundaries, i.e.  $z = 0$  and  $z = -d$ .

The matching at  $z = 0$  was already discussed in section 7. Thus, the upper exterior solution, i.e. for  $z \geq 0$ , is the Rindler's space-time

$$ds^2 = -(1 + g_u z)^2 dt^2 + dx^2 + dy^2 + dz^2,$$

$$-\infty < t < \infty, \quad -\infty < x < \infty, \quad -\infty < y < \infty, \quad 0 \leq z < \infty, \quad (67)$$

which describes a homogeneous gravitational field  $-g_u$  in the vertical (i.e.,  $z$ ) direction. And, according to (51), we see that the continuity of  $\partial_z g_{tt}$  at the upper boundary yields

$$g_u = \sqrt{6\pi\rho}(\kappa_{\text{crit}} - \kappa), \quad (68)$$

which relates the upper external gravitational field  $g_u$  with matter density  $\rho$  and  $\kappa$ . By using (61), we can also write it in terms of  $d$  and  $\rho$

$$g_u = \frac{\sqrt{6\pi\rho}}{\sin(\sqrt{6\pi\rho}d)} \left( {}_2F_1\left(-\frac{1}{2}, -\frac{1}{6}; \frac{1}{2}; \sin^2(\sqrt{6\pi\rho}d)\right) - \cos^{\frac{1}{3}}(\sqrt{6\pi\rho}d) \right). \quad (69)$$

At the lower boundary, we have  $g_{tt}(-d) = -\mathcal{G}(-d)^2 = -1$ ,  $g_{xx}(-d) = g_{yy}(-d) = \cos^{\frac{4}{3}}(\sqrt{6\pi\rho}d)$ , and  $p(-d) = 0$ .

On the other hand, regarding the derivatives, since  $\mathcal{G}(z)|_{u=u_0} = 1$  and  $p(z)|_{u=u_0} = 0$ , from (9) we get

$$\mathcal{G}'(z)|_{u=u_0} = -\frac{1}{2}V'(z)|_{u=u_m} = -\frac{\sqrt{6\pi\rho}}{3} \cot u_0 = -\frac{\sqrt{6\pi\rho}}{3} \tan(\sqrt{6\pi\rho}d), \quad (70)$$

where we have made use of (13) and (60). Thus,

$$\partial_z g_{tt}(-d)|_{\text{interior}} = -2 \mathcal{G}(-d) \mathcal{G}'(-d) = 2 \frac{\sqrt{6\pi\rho}}{3} \tan(\sqrt{6\pi\rho} d). \quad (71)$$

While from (66), we get

$$\partial_z g_{xx}(-d)|_{\text{interior}} = \partial_z g_{yy}(-d)|_{\text{interior}} = 4 \frac{\sqrt{6\pi\rho}}{3} \cos^{\frac{1}{3}}(\sqrt{6\pi\rho} z) \sin(\sqrt{6\pi\rho} d). \quad (72)$$

Taking into account the discussion in section 4, we can write the corresponding lower exterior solution, i.e. for  $z < -d$ , as

$$ds^2 = -(1 + 3g_l(d+z))^{-\frac{2}{3}} dt^2 + C_d (1 + 3g_l(d+z))^{\frac{4}{3}} (dx^2 + dy^2) + dz^2, \\ -\infty < t < \infty, \quad -\infty < x < \infty, \quad -\infty < y < \infty, \quad -d - \frac{1}{3g_l} < z \leq -d, \quad (73)$$

which describes a homogeneous gravitational field  $+g_l$  in the vertical direction and finishes up at an empty singular boundary at  $z = -d - \frac{1}{3g_l}$ .

Since  $g_{tt}(-d)|_{\text{exterior}} = -1$  and  $g_{xx}(-d)|_{\text{exterior}} = g_{yy}(-d)|_{\text{exterior}} = C_d$ , we see that, taking into account (45), the continuity of the metric components is assured if we set  $C_d = \cos^{\frac{4}{3}}(\sqrt{6\pi\rho} d)$ . And, concerning the derivatives of metric's components, we have

$$\partial_z g_{tt}(z)|_{\text{exterior}} = 2g_l (1 + 3g_l(d+z))^{-\frac{5}{3}}. \quad (74)$$

Therefore, by comparing with (71), we see that the continuity of  $\partial_z g_{tt}$  at the lower boundary yields

$$g_l = \frac{\sqrt{6\pi\rho}}{3} \tan(\sqrt{6\pi\rho} d), \quad (75)$$

which relates the lower external gravitational field  $g_l$  with  $d$  and  $\rho$ .

On the other hand, we get from (73)

$$\partial_z g_{xx}(z)|_{\text{exterior}} = \partial_z g_{yy}(z)|_{\text{exterior}} = 4 \cos^{\frac{4}{3}}(\sqrt{6\pi\rho} d) g_l (1 + 3g_l(d+z))^{\frac{1}{3}}. \quad (76)$$

Taking into account (75), by comparing the last equation with (72), we see that the matching is complete.

This solution is remarkably asymmetric, not only because both external gravitational fields are different, as we can readily see by comparing (69) and (75) (see also Fig.5), but also because the nature of vacuums is completely different: the upper one is flat and semi-infinite, whereas the lower one is curved and finishes up down bellow at an empty repelling boundary where space-time curvature diverges.

This exact solutions clearly show how the attraction of distant matter can shrink the space-time in such a way that it finishes at an empty singular boundary, as pointed out in <sup>1</sup>.

Free particles or photons move in the lower vacuum ( $-d - \frac{1}{3g_l} < z < -d$ ) along the time-like or null geodesics discussed in detail in <sup>1</sup>. So, all geodesics start and finish at the boundary of the slab and have a turning point. Non-vertical geodesics reach a turning point at a finite distance from the singularity (at  $z = -d - \frac{1}{3g_l}$ ),

and the smaller their horizontal momentum is, the closer they get the singularity. The same occurs for vertically moving particles, i. e., the higher the energy, the closer they approach the singularity. Only vertical null geodesics just touch the singularity and bounce (see Fig. 1 of Ref. <sup>1</sup> upside down).

### 8. The Newtonian limit and the restoration of the mirror symmetry

It should be noted that the solutions so far discussed are mirror-asymmetric. In fact, it has been shown in <sup>6</sup> that the solution cannot have a “plane” of symmetry in a region where  $p(z) \geq 0$ . In order to see this, suppose that  $z = z_s$  is that “plane”, then it must hold that  $\mathcal{G}' = V' = p' = 0$  at  $z_s$ , and so from (9) we get that also  $p(z_s) = 0$ , and then  $\mathcal{G}(z_s) = 1$ . Now, by differentiating (10) and using (32), we obtain  $p''(z_s) = -4\pi\rho^2 < 0$ .

Notice that (13) and the condition  $V'(z_s) = 0$  imply that  $u = \pi/2$ . And then we get from (34) that the condition  $\mathcal{G}'(z_s) = 0$  implies  $\kappa = \kappa_{\text{crit}}$ .

Therefore, the only mirror symmetric solution is the joining of two identical neutral slabs discussed in section 6. We clearly get from (44), that for this solution we have

$$\mathcal{G}(z) = \frac{{}_2F_1\left(-\frac{1}{2}, -\frac{1}{6}; \frac{1}{2}; \sin^2(\sqrt{6\pi\rho}z)\right)}{(1 - \sin^2(\sqrt{6\pi\rho}z))^{1/6}}, \quad (77)$$

which shows that it is a  $C^\infty$  even function of  $z$  in  $-\sqrt{\frac{\pi}{24\rho}} < z < \sqrt{\frac{\pi}{24\rho}}$ . But, of course, we have seen in section 2 that  $-\rho \leq p(z) \leq 0$  in this case.

However, for the solution of the preceding section, this asymmetry turns out to disappear when  $\sqrt{6\pi\rho}d \ll 1$ . In fact, from (69) we get

$$g_u = 2\pi\rho d(1 + \frac{2}{3}\pi\rho d^2 + \dots) \text{ for } \sqrt{6\pi\rho}d < 1, \quad (78)$$

while from (75) we get

$$g_l = 2\pi\rho d(1 + 2\pi\rho d^2 + \dots) \text{ for } \sqrt{6\pi\rho}d < 1. \quad (79)$$

Hence, both gravitational fields tend to the Newtonian result  $2\pi\rho d$ , and the difference between them is of the order  $(\sqrt{6\pi\rho}d)^3$ .

Furthermore, in this limit, (65) becomes

$$\mathcal{G}(z) = 1 + 2\pi\rho z(z+d) + \frac{4}{3}\pi^2\rho^2 z(z^3+d^3) + O((\sqrt{6\pi\rho}d)^6), \quad (80)$$

so

$$g_{tt}(z) = -\mathcal{G}(z)^2 \approx -(1 + 4\pi\rho z(z+d)), \quad (81)$$

which shows that the Newtonian potential inside the slab tends to

$$\Phi(z) = 2\pi\rho z(z+d). \quad (82)$$

Since  $\Phi(-\frac{d}{2} - z) = \Phi(-\frac{d}{2} + z)$ , it is mirror-symmetric at  $z = -d/2$ .

Moreover, we obtain from (11) that the pressure inside the slab tends to the hydrostatic Newtonian result

$$p(z) = -2\pi\rho^2 z(z + d). \quad (83)$$

It should also be noted, by comparing (38) and (62), that in this limit, they lead to

$$\frac{p_m}{\rho} = \frac{\pi\rho}{2} d^2. \quad (84)$$

Therefore, in the Newtonian limit, the the mirror symmetry at the middle point of the slab is restored.

## 9. Thinner Repelling Slabs

By exchanging the place of matter and vacuum, we can also match the piece of the interior solution discarded in section 7 to the discarded asymptotically flat tail of Taub's vacuum, thus getting a repulsive slab.

Clearly, the inner solution is given by (66), but now  $-\sqrt{\frac{\pi}{24\rho}} < z \leq -d$ . While the outer one is given by (73) with  $-d \leq z$ . Therefore, we get from (75)

$$g = \frac{\sqrt{6\pi\rho}}{3} \tan(\sqrt{6\pi\rho}d), \quad (85)$$

which relates the external gravitational field  $g$  with  $d$  and  $\rho$ . But now, the thickness of this slab is

$$d' = \sqrt{\frac{\pi}{24\rho}} - d < \sqrt{\frac{\pi}{24\rho}}, \quad (86)$$

and so

$$g = \frac{\sqrt{6\pi\rho}}{3} \cot(\sqrt{6\pi\rho}d'). \quad (87)$$

Of course, by means of (27), (65) and (86),  $\mathcal{G}(z)$  and  $p(z)$  can also be explicitly written down in terms of  $d'$  and  $\rho$  in this case.

In this repulsive case, free particles or photons move in the vacuum ( $z > 0$ ) along the mirror image of time-like or null geodesics discussed in detail in <sup>1</sup>. All occurs in the vacuum as if there were a Taub singularity inside the matter at a distance  $|1/3g|$  from the surface—this image singularity should not be confused with the “real” inner one situated  $d'$  from the surface. Therefore, only the Taub's geodesics for which the distance between the turning point and the image singularity is smaller than  $\frac{1}{3g}$ , should be cut at slab's surface. For instance, this always occurs for vertical photons. These facts are easily seen by looking at Fig. 1 of reference <sup>1</sup> upside down and by exchanging the position of vacuum and matter.

Notice that these slabs turn out to be less repulsive than the ones discussed in section 5, since all incoming vertical null geodesics reach the slab surface in this case.

## 10. Concluding remarks

We have done a detailed study of the exact solution of Einstein's equations corresponding to a static and plane symmetric distribution of matter with constant positive density. By matching this internal solution to vacuum ones, we showed that different situations arise depending on the value of a parameter  $\kappa$ .

We found that the dominant energy condition is satisfied only for  $\kappa \geq \kappa_{dec} = 0.3513\dots$

As a result of the matching, we get very simple complete (matter and vacuum) exact solutions presenting some somehow astonishing properties without counterpart in Newtonian gravitation:

The maximum depth that these slabs can reach is  $\sqrt{\frac{\pi}{24\rho}}$  and the solutions turn out to be remarkably asymmetric.

We found repulsive slabs in which negative but bounded ( $|p| \leq \rho$ ) pressure dominate the attraction of the matter. These solutions finish deep below at a singularity where  $p = -\rho$ . If their depth is smaller than  $\sqrt{\frac{\pi}{24\rho}}$ , the exterior is the asymptotically flat tail of Taub's vacuum plane solution, while when they reach the maximum depth the vacuum turns out to be a flat Rindler space-time with event horizons, showing that there are incoming vertical photons which never reach the surface of the slabs in this case.

We also found attractive solutions finishing deep below at a singularity. In this case the outer solution in this case is a Rindler space-time.

We also described a non-singular solution of thickness  $d$  surrounded by two vacuums. This solution turns out to be attractive and remarkably asymmetric because the nature of both vacuums is completely different: the "upper" one is flat and semi-infinite, whereas the "lower" one is curved and finishes up down below at an empty repelling boundary where space-time curvature diverges. The pressure is positive and bounded, presenting a maximum at an asymmetrical position between the boundaries. We explicitly wrote down the pressure and the external gravitational fields in terms of  $\rho$  and  $d$ . We show that if  $0 < \sqrt{6\pi\rho}d < 1.52744\dots$ , the dominant energy condition is satisfied all over the space-time. We also show how the mirror symmetry is restored at the Newtonian limit. These exact solutions clearly show how the attraction of distant matter can shrink the space-time in such a way that it finishes at an empty singular boundary, as pointed out in <sup>1</sup>.

We have also discussed matching an attractive slab to a repulsive one, and two neutral ones. We also comment on how to assemble relativistic gravitational capacitors consisting of a slice of vacuum trapped between two such slabs.

### Appendix: Some properties of ${}_2F_1(a, b; c; x)$

Here, we show how the integral appearing in the first line of (16) is performed. By doing the change of variable  $t = \sin^2 u'$ , we can write

$$\int_0^u \sin^a u' \cos^b u' du' = \frac{1}{2} \int_0^{\sin^2 u} t^{\frac{a-1}{2}} (1-t)^{\frac{b-1}{2}} dt = \frac{1}{2} B_{\sin^2 u} \left( \frac{a+1}{2}, \frac{b+1}{2} \right), \quad (88)$$

where  $B_x(p, q)$  is the incomplete beta function, which is related to a hypergeometric function through

$$B_x(p, q) = \frac{x^p}{p} {}_2F_1(p, 1-q; p+1; x) \quad (89)$$

(see for example <sup>12</sup>). Therefore,

$$\begin{aligned} \int_0^u \sin^a u' \cos^b u' du' &= \frac{(\sin u)^{a+1}}{a+1} {}_2F_1\left(\frac{a+1}{2}, \frac{1-b}{2}; \frac{a+3}{2}; \sin^2 u\right) \\ &= \frac{1}{a+1} (\sin u)^{a+1} (\cos u)^{b+1} {}_2F_1\left(1, \frac{a+b+2}{2}; \frac{a+3}{2}; \sin^2 u\right), \end{aligned} \quad (90)$$

where we used the transformation  ${}_2F_1(a, b; c; x) = (1-x)^{c-a-b} {}_2F_1(c-a, c-b; c; x)$  in the last step.

For the sake of completeness, we display here the very few formulas involving hypergeometric functions  ${}_2F_1(a, b; c; z)$  required to follow through all the steps of this paper.

As it is well known

$${}_2F_1(a, b; c; z) = 1 + \frac{ab}{c}z + \frac{a(a+1)b(b+1)}{c(c+1)} \frac{z^2}{2!} + \dots, \quad \text{for } |z| < 1. \quad (91)$$

By using the transformation <sup>12,13</sup>

$$\begin{aligned} {}_2F_1(a, b; c; z) &= \frac{\Gamma(c)\Gamma(c-a-b)}{\Gamma(c-a)\Gamma(c-b)} {}_2F_1(a, b; a+b-c+1; 1-z) \\ &+ (1-z)^{c-a-b} \frac{\Gamma(c)\Gamma(a+b-c)}{\Gamma(a)\Gamma(b)} {}_2F_1(c-a, c-b; c-a-b+1; 1-z), \end{aligned} \quad (92)$$

with  $a = -1/2$ ,  $b = -1/6$ , and  $c = 1/2$ , we find the useful relations

$$\frac{3}{7} (1-z)^{\frac{7}{6}} {}_2F_1\left(1, \frac{2}{3}; \frac{13}{6}; 1-z\right) = -\frac{\sqrt{\pi}\Gamma(\frac{7}{6})}{\Gamma(\frac{2}{3})} \sqrt{z} + {}_2F_1\left(-\frac{1}{2}, -\frac{1}{6}; \frac{1}{2}; z\right) \quad (93)$$

$$= -\frac{\sqrt{\pi}\Gamma(\frac{7}{6})}{\Gamma(\frac{2}{3})} \sqrt{z} + 1 + \frac{z}{6} + \frac{5z^2}{216} + \frac{11z^3}{1296} + \dots, \quad \text{for } |z| < 1, \quad (94)$$

or, by making  $z \rightarrow 1-z$ ,

$${}_2F_1\left(-\frac{1}{2}, -\frac{1}{6}; \frac{1}{2}; 1-z\right) = \frac{\sqrt{\pi}\Gamma(\frac{7}{6})}{\Gamma(\frac{2}{3})} \sqrt{1-z} + \frac{3}{7} z^{\frac{7}{6}} {}_2F_1\left(1, \frac{2}{3}; \frac{13}{6}; z\right) \quad (95)$$

$$= \frac{\sqrt{\pi}\Gamma(\frac{7}{6})}{\Gamma(\frac{2}{3})} \sqrt{1-z} + \frac{3}{7} z^{\frac{7}{6}} \left(1 + \frac{4z}{13} + \frac{40z^2}{247} + \frac{128z^3}{1235} + \dots\right), \quad \text{for } |z| < 1. \quad (96)$$

**References**

1. Gamboa Saraví, R. E.: *Int. J. Mod. Phys. A* **23**, 1995 (2008); Errata: *Int. J. Mod. Phys. A* **23**, 3753 (2008).
2. Gamboa Saraví, R. E.: *Class. Quantum Grav.* **25** 045005 (2008).
3. Gamboa Saraví, R. E.: *Gen. Rel. Grav.* in press. Preprint arXiv:0709.3276 [gr-qc].
4. Taub, A. H.: *Phys. Rev.* **103** 454, (1956).
5. Avakyan, R. M., Horský, J.: *Sov. Astrophys. J.* **11**, 454, (1975).
6. Novotný, J., Kucera, J., Horský, J.: *Gen. Rel. Grav.* **19**, 1195. (1987).
7. Stephani, H., Kramer, D., MacCallum, M., Hoenselaers, C., Herlt, E.: *Exact Solutions to Einstein's Field Equations*, Second edition, Cambridge Univ. Press (2003).
8. Schwarzschild, K.: *Sitzber. Deut. Akad. Wiss. Berlin, Kl. Math.-Phys. Tech.*, 424 (1916).
9. Taub, A. H.: *Ann. Math.* **53** 472, (1951).
10. Novotný, J., Horský, J.: *Czech. J. Phys. B* **24**, 718 (1974).
11. Gamboa Saraví, R. E.: in preparation.
12. Gradshteyn, I. S., Ryzhik, I. M.: *Table of Integrals, Series, and Products*, Academic Press Inc. (1963).
13. Abramowitz, M., Stegun, I. A., eds.: *Handbook of Mathematical Functions with Formulas, Graphs, and Mathematical Tables*. New York: Dover, 1972.